JOURNAL OF GEOPHYSICAL RESEARCH, VOL. 112, D19304, doi:10.1029/2007JD008844, 2007

Water-soluble species in the marine aerosol from the northern South China Sea: High chloride depletion related to air pollution

Shih-Chieh Hsu,[1] Shaw Chen Liu,[1,2] Shuh-Ji Kao,[1] Woei-Lih Jeng,[3] Yi-Tang Huang,[1,3]
Chun-Mao Tseng,[3] Fujung Tsai,[1] Jien-Yi Tu,[1] and Yih Yang[4]

Received 18 April 2007; revised 10 June 2007; accepted 21 June 2007; published 9 October 2007.

[1] Dichotomous ($PM_{2.5-10}$ and $PM_{2.5}$ modes) and size-resolved marine aerosols collected during the northeastern monsoon on two wintertime cruises in the subtropical South China Sea (SCS) were analyzed for water-soluble ions. During the sampling periods the study region was under the influence of strong pollution originating primarily from the Asian continent. Elevated levels of non-sea-salt sulfate and ammonium ions of up to 4.5 and 1.2 $\mu g/m^3$, respectively, were observed, indicating that the SCS is now substantially contaminated by massive amounts of air pollutants most likely from China and South/Southeast Asia. The non-sea-salt sulfate to nitrate mass ratios reaching 3.8 ± 1.9 are much larger than those (approximately 2) in and around East Asia and the western Pacific Ocean, suggesting that the Asian outflow aerosols measured in the SCS experienced different traveling history from those in the vicinity of source regions. High chloride depletion (Cl-depletion) measured in the SCS marine aerosols was, on average, 30% for coarse-mode particles and nearly 90% for fine-mode particles. Cl-depletion is size-dependent, and maximizes in submicrometer particles (i.e., Cl has almost been completely lost). Acid displacement is responsible for the observed high Cl-depletion: nitrate substitution accounts for the coarse-mode depletion, whereas sulfate substitution accounts for the fine-mode depletion. The acid displacement of sea salt aerosols may be related to a variety of factors, especially the substantial air pollution, which is discussed in detail in this paper. On cloudy/rainy days, fine-mode aerosol samples have moderate Cl-depletion (i.e., ~40–50%), in contrast to nearly complete Cl loss on sunny days, presumably indicating that photochemical reactions would play a key role in the Cl-deficit; however, it merits further investigation as the available samples were limited.

Citation: Hsu, S.-C., S. C. Liu, S.-J. Kao, W.-L. Jeng, Y.-T. Huang, C.-M. Tseng, F. Tsai, J.-Y. Tu, and Y. Yang (2007), Water-soluble species in the marine aerosol from the northern South China Sea: High chloride depletion related to air pollution, *J. Geophys. Res.*, *112*, D19304, doi:10.1029/2007JD008844.

1. Introduction

[2] It is well documented that sea salt aerosols can participate in heterogeneous reactions with nitric and sulfuric acids, leading to chloride (and also other halogens like Br) depletion (hereafter denoted by Cl-depletion) through HCl volatilization (and the production of halogen radials), particularly in relatively polluted marine air [*Sturges and Shaw*, 1993; *Johansen et al.*, 1999]. As a result, this may be an important removal process of pollutant species like nitrogen and sulfur and in turn may cause changes in the physicochemical, oxidative, and optical properties of aerosol particles in the marine boundary layer [*Fan and Jacob*, 1992]. Also, the halogens Cl and Br that mobilize from sea salt particulate forms to reactive gaseous forms are implicated in playing a major role in destroying light hydrocarbons and in atmospheric ozone depletion, particularly in the polar oceans [*Jobson et al.*, 1994; *Vogt et al.*, 1996]. The magnitude of Cl-depletion of marine aerosols has been demonstrated to be usually dependent on particle size, i.e., increasing with decreasing size [*Yao et al.*, 2003]. Although the primary controlling factors have been well understood [e.g., *Song and Carmichael*, 1999; *Maxwell-Meier et al.*, 2004; *Quinn and Bates*, 2005], certain mechanisms governing the differential Cl loss of sea salt particles in diverse oceanic regions still require investigation. *Johansen et al.* [1999] have observed large variances of Cl-deficit between samples and seasons, and the differences in Cl-deficit between seasons did not match the differences in the levels

---

[1] Research Center for Environmental Changes, Academia Sinica, Taipei, Taiwan.

[2] Department of Atmospheric Sciences, National Taiwan University, Taipei, Taiwan.

[3] Institute of Oceanography, National Taiwan University, Taipei, Taiwan.

[4] National Center of Oceanographic Research, National Taiwan University, Taipei, Taiwan.

Copyright 2007 by the American Geophysical Union.
0148-0227/07/2007JD008844$09.00

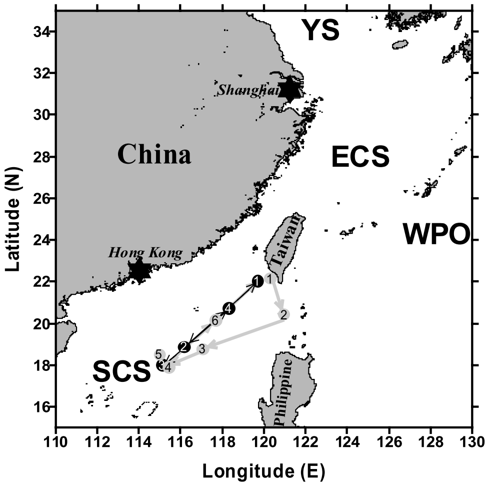

Figure 1. A regional map showing the ship's track (from Kaohsiung to SEATS site (18.25°N; 115.67°E) back to Kaohsiung) for the two research cruises conducted in the South China Sea in November 2004 (thick gray line) and January 2005 (thin black line). The number (n) in the circle indicates the nth sample collected during each cruise, which is marked at the beginning of a given segment corresponding to the track where individual samples were collected. SCS: South China Sea; YS: Yellow Sea; ECS: East China Sea; and WPO: western Pacific Ocean.

of anthropogenic species (like Pb, anthropogenic sulfate and nitrate). Assuming only the levels of anthropogenic sulfate and nitrate responsible for the phenomenon, they thus argued that certain mechanisms of acid displacement have not yet been recognized.

[3] The South China Sea (SCS) is the largest basin in the tropical-subtropical western North Pacific (Figure 1). The prevailing winds in the summer are southerly and southwesterly, yet in winter and spring, northerly and northeasterly winds prevail. The annual average temperature is about 25°C, and the rainfall is around 2000 mm; thus the SCS is characterized by warm, moist weather. In southern China, high concentrations of various reactive trace gases (e.g., SO_2 and NO_y) were observed, with an evident seasonality of wintertime maxima and summertime minima [*Wang et al.*, 2005]. Asian dust and air pollutants from northern China can even travel a great distance southward around northern Taiwan, frequently during the northeast monsoon [*Hsu et al.*, 2004, 2006]. It is reasonable to expect that the SCS would receive massive quantities of pollutants and dust from northern China's deserts and arid areas. Biomass burning particles from South/Southeast Asia may contribute additional anthropogenic constituents [*Ma et al.*, 2003, and references therein], particularly during the southern monsoon. These natural and anthropogenic aerosol particles may alter the marine aerosol chemical composition and atmospheric chemistry of the SCS. However, few measurements on chemical characteristics of the SCS marine aerosols have been documented [*Ma et al.*, 2003, 2005]. Particularly, from Transport and Chemical Evolution over the Pacific (TRACE-P) springtime measurement campaigns [*Ma et al.*, 2003], strong biomass burning plumes have been observed at an altitude of 3 km in and around the northern SCS, which was identified by the combinations of high fine potassium and air mass trajectory analysis. The plumes originated from Southeast Asia and dispersed over the study region. Here we present chemical data on the water-soluble ion compositions of aerosols in the marine boundary layer in the northern SCS (Figure 1) during the winter (northeast) monsoon.

2. Materials and Methods

[4] Marine aerosol samples were collected during two research cruises (Figure 1) on board the R/V *Ocean Researcher I* from 5 to 11 November 2004 (six sets of dichotomous samples and one set of size-resolved samples) and from 20 to 24 January 2005 (four sets of dichotomous samples and one set of size-resolved samples) during the strongest northeast monsoon, with a mean wind speed of approximately 6 m/sec. Meteorological data (including air temperature, wind speed and direction, and atmospheric pressure) were measured by the on-board system. Cloudy to showery weather was recorded on 2 days: 9 November 2004 and 21 January 2005. Aerosol samplers were set up on the upper foredeck (14 m above sea level). Daily dichotomous samples of particle sizes of <2.5 and 2.5–10 μm (hereafter referred to as $PM_{2.5}$ and $PM_{2.5-10}$, respectively) were collected with a dichotomous sampler (Thermo Andersen SA241) for approximately 24 hours, except for samples collected on the first and last days of each cruise. One set of size-segregated samples, covering the whole cruise period, was collected from each cruise. The size-segregated aerosol sample was collected using a 10-stage micro-orifice uniform deposit impactor (MOUDI, Model 110, MSP Corporation, Minneapolis, Minnesota, United States). This sampler has 10 size-fractionated stages (50% cut-off diameters: 10, 5.6, 2.5, 1.8, 1.0, 0.56, 0.32, 0.18, 0.10, and 0.056 μm) with inlet (nominal cut-size 18 μm) and backup (<0.018 μm) filters; the flow rate was controlled at 30 l/min. The filtrating substrates were 37 mm diameter PTFE membrane filters (pore size 1.0 μm, PallGelman) for dichotomous samples and 47 mm diameter PTFE membrane filters (pore size 1.0 μm, PallGelman) for size-resolved samples on all stages except on the backup filter, where quartz filters were used, and thus these samples were not analyzed. The inclusion of the inlet stage allowed collections of particles in 11 size fractions between 0.056 and >18 μm. Teflon filters were stored in airtight individual petridishes before and after sampling to avoid contamination. Filters were dried in a dry box for at least 48 hours before weighing and then weighed using a microbalance (MX 5, Mettler-Toledo Incorporated; detection limit 1 μg) in a weighing room at a relative humidity of $\leq$35%.

[5] Aerosol-laden filter samples were ultrasonically extracted for the water-soluble inorganic species with Milli-Q water (specific resistivity 18.2Ω; Millipore Corporated, Massachusetts, United States). Analysis of extract solutions was performed with an ion chromatograph (Dionex ICS-90 and ICS-1500) equipped with a conductivity detector (ASRS-ULTRA). A Dionex AS9-HC separator column was used for analyzing Cl^-, NO_3^- and SO_4^{2-}, and a CS12A separator column for analyzing Na^+ and NH_4^+. The eluents used were 9 mM Na_2CO_3 for anions and 20 mM methansul-

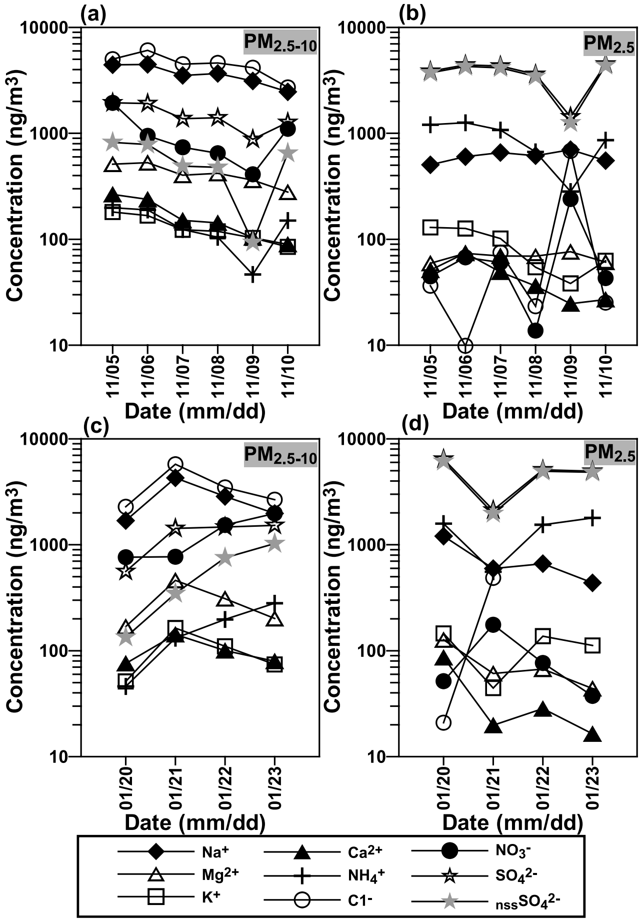

Figure 2. Time series of water-soluble ions Na^+ (solid diamonds), Mg^{2+} (open triangles), K^+ (open squares), Ca^{2+} (solid triangles), NH_4^+ (plus signs), Cl^- (open circles), NO_3^- (solid circles), SO_4^{2-} (open stars), and $_{nss}SO_4^{2-}$ (solid stars) in $PM_{2.5\text{-}10}$ (left) and $PM_{2.5}$ (right) marine aerosols from two cruises, November 2004 (top) and January 2005 (bottom).

fonic acid (MSA) for cations. In general, detection limits for dichotomous samples were within 0.01 μgm^{-3} for all ions except Cl^- (around 0.015 μgm^{-3}), while for size-resolved samples with much more filtered air volume they can be reduced by a factor of about eight. For cations of the metals Na, Mg, K, and Ca the samples were analyzed using ICP-MS (Elan 6100, Perkin-Elmer™ Instruments, United States) while for Na the samples were analyzed with two instruments (IC and ICP-MS), obtaining a consistent result of <10% difference. Detection limits for cations are within 0.002 μgm^{-3}, except for Ca (0.006 μgm^{-3}) in dichotomous samples; similarly, detection limits can be reduced by a factor of eight for size-resolved samples. The details of ICP-MS analysis are given elsewhere [*Hsu et al.*, 2004].

[6] The Lagrangian integrated model HYSPLIT 4 based on the FNL global wind field was used for illustrating the possible air mass trajectories (NOAA Air Resources Laboratory (http://www.arl.noaa.gov/ready/open/hysplit4.html)). The concentration of non-sea-salt SO_4^{2-} ($_{nss}SO_4^{2-}$) sulfate was calculated by subtracting sea salt SO_4^{2-} ($_{ss}SO_4^{2-}$) from total SO_4^{2-}, of which $_{ss}SO_4^{2-}$ was estimated by multiplying Na^+ by a factor of 0.252, where the coefficient of 0.252 is a typical sulfate-to-sodium mass ratio in seawater.

3. Results and Discussion

3.1. Concentration Levels and Size Distribution of Major Water-Soluble Ions

[7] Time series of atmospheric concentrations for the analyzed major water-soluble ions in two size modes of marine aerosols from the northern SCS are displayed in Figure 2 and statistically summarized in Table 1. A comparison of our data with the only data set ever reported for the SCS [*Ma et al.*, 2005] shows that they are very comparable for most ions. When compared with results from the East China Sea (ECS), the present concentration levels for anthropogenic constituents such as $_{nss}SO_4^{2-}$ (average 4.5 $\mu g/m^3$, with a certain portion of biogenic contributions), NO_3^- (1.2 $\mu g/m^3$), and NH_4^+ (1.2 $\mu g/m^3$) appear to be moderate (approximately one half of the ECS mean concentrations) during the same polluted, northeastern monsoon time frame [*Bates et al.*, 2004; *Nakamura et al.*, 2005]. Results with $_{nss}SO_4^{2-}$ and NH_4^+ as high as 7 and 2 $\mu g/m^3$, respectively, indicate that while located farther from the major continent than the ECS, the SCS atmosphere receives, at times, substantial pollution as such concentration levels are much higher than those measured in many remote oceans [*Matsumoto et al.*, 1998; *Prospero and Savoie*, 2003]. Furthermore, we compared our data with the results from the mission flight 10 of the TRACE-P campaign conducted in Luzon Strait located at the same latitude as our study ocean in early spring [see *Ma et al.*, 2003, Figure 3]. For SO_4^{2-}, both had comparable concentrations (5–6 $\mu g/m^3$) in the marine boundary layer, while NH_4^+ was lower in the SCS than in Luzon Strait (2–3 $\mu g/m^3$) by a factor of 1–2. For fine-mode NO_3^- and K^+, they were similarly low (Table 1), consistent with the values of the TRACE-P (~0.5 $\mu g/m^3$ for NO_3^-, and certain very low values for K^+ that cannot be readily read from their figure). On average, $_{nss}SO_4^{2-}$ accounts for 40% and 96% of the total SO_4^{2-} for the coarse- and fine-mode aerosols, respectively. In the case of Cl^- and Na^+ that predominantly originate from sea spray, values (averaging ~4 $\mu g/m^3$) are quite consistent with the only literature data set available for the SCS [*Ma et al.*, 2005] and also with those observed in the marine boundary layer of remote oceans [*Quinn and Bates*, 2005].

[8] Note that the coarse-mode fraction dominates the total NO_3^- [*Quinn and Bates*, 2005], similar to the sea salt ions represented by Na^+ and Cl^- (Table 1). Overall, the levels of atmospheric concentrations for anthropogenic species such as $_{nss}SO_4^{2-}$ and NH_4^+ are essentially dependent on the origins (continental or maritime) of the air masses collected. This relationship can be identified by the 5-day air mass backward trajectory analysis using the HYSPLIT model (Figure 3). For instance, during the November cruise, continental air masses dominated from the 5th to 7th day, while maritime air masses dominated from the 8th to 10th day. This temporal variability for all anthropogenic species (SO_4^{2-}, NH_4^+ and NO_3^-, but not for fine-mode NO_3^-) (Figures 2a and 2b) declined from a high level on 5 November to a minimum on 9 November when maritime air masses dominated, corresponding reasonably well with the air mass

Table 1. A Summary for the Range and Mean (±One Standard Deviation) of Atmospheric Concentrations (Equivalent Concentrations) for Major Water-Soluble Ions[a]

	$PM_{2.5-10}$		$PM_{2.5}$		PM_{10}	
	Range	Mean ± S.D.	Range	Mean ± S.D.	Range	Mean ± S.D.
Na^+	1692–4473[b] (74–194[c])	3250 ± 1003 (141 ± 44)	438–1205 (19–52)	654 ± 209 (28 ± 9.1)		-
Mg^{2+}	169–528 (14–43)	365 ± 124 (30 ± 10)	44–127 (3.6–10)	71 ± 22 (5.8 ± 1.8)		-
K^+	51–181 (1.3–4.6)	118 ± 43 (3.0 ± 1.1)	38–146 (1.0–3.7)	95 ± 41 (2.4 ± 1.1)		-
Ca^{2+}	76–265 (3.8–13)	139 ± 65 (6.9 ± 3.3)	16–86 (0.8–4.3)	41 ± 24 (2.1 ± 1.2)		-
NH_4^+	46–281 (2.6–16)	147 ± 73 (8.2 ± 4.0)	282–1795 (16–100)	1083 ± 490 (60 ± 27)		-
Cl^-	2284–6072 (64–171)	4126 ± 1314 (116 ± 37)	10–682 (ND–19.2)	170 ± 262 (3.8 ± 6.8)		-
NO_3^-	410–1978 (6.6–32)	1084 ± 549 (17 ± 8.9)	14–240 (0.2–3.9)	81 ± 71 (1.3 ± 1.1)		-
SO_4^{2-}	560–1940 (12–40)	1377 ± 417 (29 ± 8.7)	1432–6433 (30–134)	4077 ± 1446 (85 ± 30)		-
${}_{nss}SO_4^{2-}$	94–1027 (2.0–21)	558 ± 305 (12 ± 6.4)	1255–6129 (26–128)	3912 ± 1426 (82 ± 30)		-
${}_{nss}SO_4^{2-}/NO_3^-$ mass ratio	0.2–0.8	0.5 ± 0.2	5–251	59 ± 70	2.1–7.7	3.8 ± 1.9

[a] Also given are the ${}_{nss}SO_4^{2-}$ to NO_3^- ratios. (n = 10).

[b] The unit is ng/m^3.

[c] The unit is neq/m^3.

origins as well as the sampling locations relative to the land. Obviously, the wintertime air mass trajectories are different from those measured in the springtime TRACE-P measurement campaigns [*Ma et al.*, 2003], when the air parcels at attitude of below 1 km came from the west–southwest (Hanoi).

[9] Also given in Table 1 are the ${}_{nss}SO_4^{2-}/NO_3^-$ mass ratios for coarse- and fine-mode aerosols. It is interesting to note that for coarse-mode particles the ratios are always less than 1.0, whereas for fine-mode particles the ratios even reach 60. Alternatively, coarse NO_3^- concentrations always exceed coarse ${}_{nss}SO_4^{2-}$; in contrast, fine ${}_{nss}SO_4^{2-}$ always

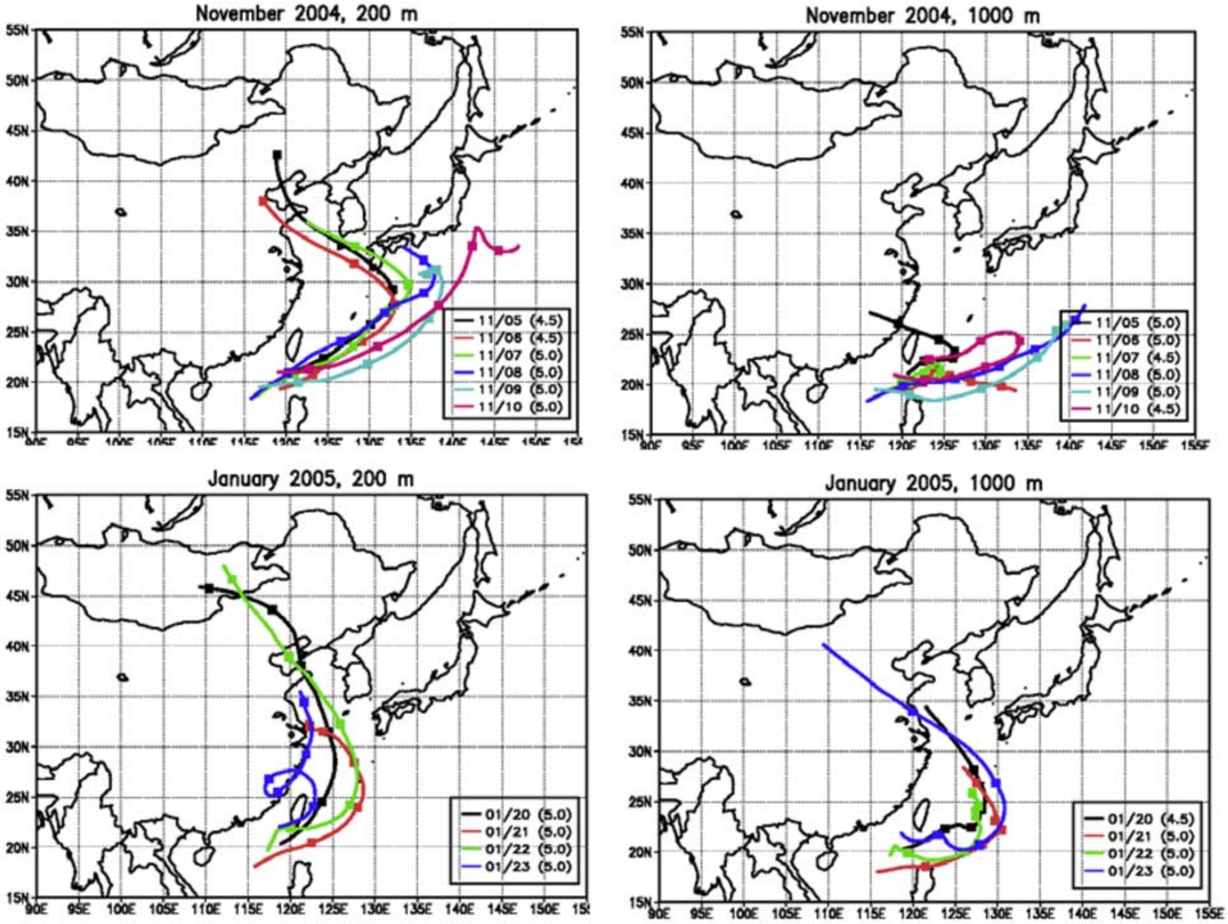

Figure 3. Five-day air mass back trajectory analyses at two altitudes (left: 200 m; right: 1000 m) for two cruise periods (top: November 2004 samples; bottom: January 2005 samples), illustrating the possible origins of the air masses. Markers on the trajectory denote position for every 24 hours. The starting time for each trajectory is at 1500 UTC each day.

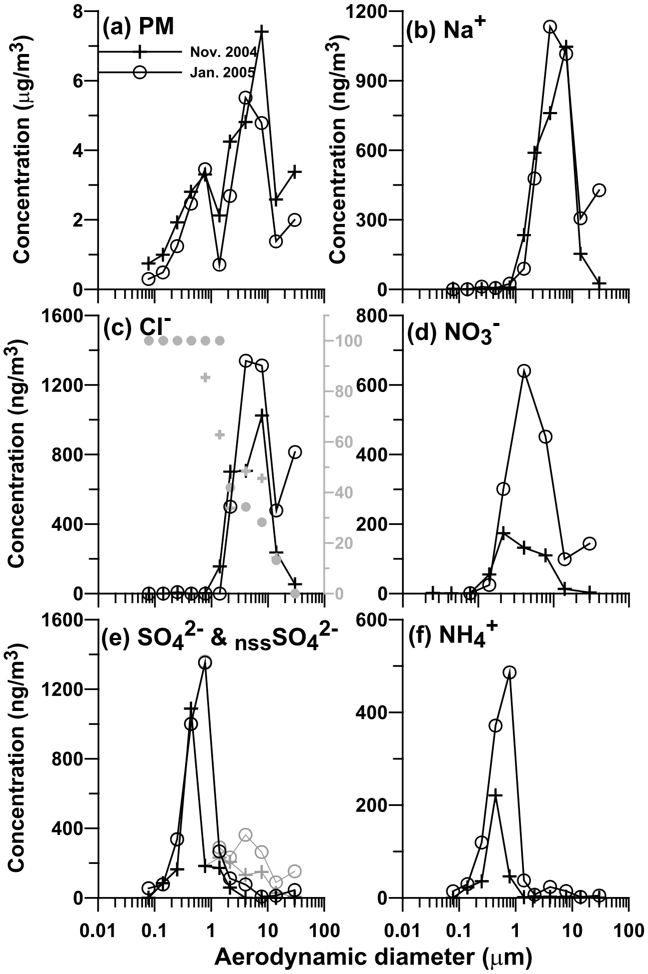

Figure 4. Mass size distribution for PM (a), Na^+ (b), Cl^- (c), NO_3^- (d), total SO_4^{2-} (black symbols), and $_{nss}SO_4^{2-}$ (gray symbols) (e) and NH_4^+ (f) for two sets of size-resolved samples (plus signs: November 2004 samples; open squares: January 2005 samples). Also given in Figure 4c is the Cl-depletion (scale in the right axis) varying with particle sizes for the two sets of samples (gray symbols). Note that the unit is μg/m3 for Figure 4a and ng/m^3 for Figure 4b.

largely exceeds fine NO_3^-. For comparison, the ratios for PM_{10} (i.e., sum of $PM_{2.5}$ and $PM_{2.5-10}$) are also given, ranging from 2.1 to 7.7 and averaging 3.8 ± 1.9. Compared to those (averaging 1.7–2.8) observed at East Asian coastal sites (including Cheju of Korea, Kato and Okinawa of Japan, and Kenting of Taiwan) and the western Pacific island sites (Midway and Oahu) [*Arimoto et al.*, 1996], the ratios observed in the tropical SCS appear to be much higher, which is a distinctive feature from the abovementioned regions. Apparently, this indicates that the partitioning of $_{nss}SO_4^{2-}$ and NO_3^- between coarse- and fine-mode marine aerosols occurs in different ways over the SCS. In other words, the Asian outflow aerosols measured in the SCS experienced different traveling history from those in the vicinity of source regions. Another important feature is that fine-mode samples have $_{nss}SO_4^{2-}$ and NH_4^+ minima and NO_3^- maxima on both 9 November 2004 and 21 January 2005 during the respective cruise periods (Figures 2b and 2d), which may be related to photochemical processes, as discussed in section 3.3.

[10] The aerosol mass size distribution for two sets of size-segregated samples shows a typically bimodal pattern. The first peak is at 5.6–10 μm (stage 3, for November 2004 samples) or 2.5–5.6 μm (stage 4, for January 2005 samples), and the second peak is at 0.56–1.0 μm (stage 7, Figure 4a). For ions Na^+ (Figure 4b), Mg^{2+} (similar to Na^+, not shown), Cl^- (Figure 4c), and NO_3^- (Figure 4d), they all show a monomode with a peak at 5.6–10 μm (stage 3) or 2.5–5.6 μm (stage 4) (except the November 2004 sample set NO_3^- peaked at 1.8–2.5 μm (stage 5)), thereby accounting for the first concentration peak of particulate matter (PM) mass. For ions SO_4^{2-} (Figure 4e) and NH_4^+ (Figure 4f), they also show a monomodal pattern but peak at 0.32–0.56 μm (stage 8) (for the November 2004 samples) or 0.56–1.0 μm (stage 7, for the January 2005 samples), thereby accounting for the second peak of PM mass. The size distribution patterns and concentration levels for these major water-soluble ions are quite similar to the only results ever previously reported for the SCS [*Ma et al.*, 2005]. Our results also show that most of NO_3^- associates within coarse-mode particles while having an insignificant amount in the fine mode. This is consistent with the results of the dichotomous samples and very similar to the patterns of sea salt particles represented by Na^+, but dissimilar to the

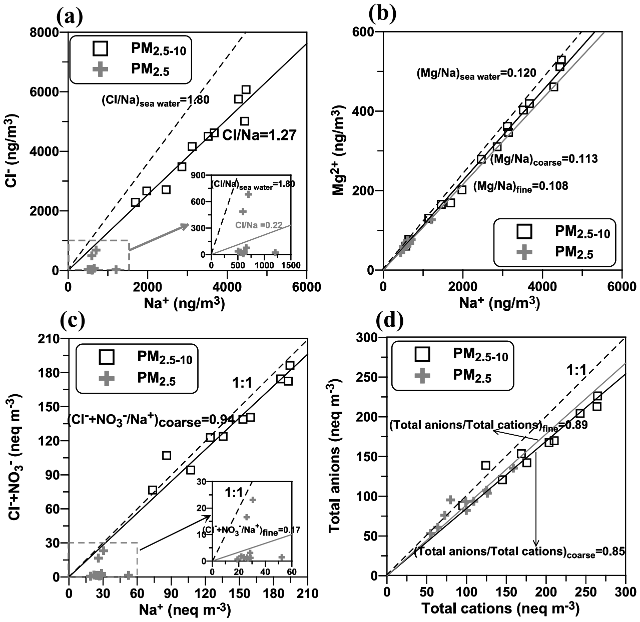

Figure 5. Relationships for Na^+ versus Cl^- (a), Na^+ versus Mg^{2+} (b), Na^+ versus $[Cl^- + NO_3^-]$ (c), and total cations versus total anions for two modes (open squares for $PM_{2.5-10}$ and gray crosses for $PM_{2.5}$) of dichotomous samples (n = 10). The parts of $PM_{2.5}$ in Figures 5a and 5c are enlarged into an inset. Also given are regression lines. Note that the unit is ng/m^3 for the two upper plots and neq/m^3 for the two lower plots.

patterns of airborne dust particles represented by Al that spikes at 1.0–1.8 μm (stage 6, not shown). The difference in size distribution between SO_4^{2-} and NO_3^- may result in their differential removal through dry deposition, more efficient for NO_3^- than for SO_4^{2-}, which thus is a primary factor leading to a much larger SO_4^{2-}/NO_3^- ratio in the SCS aerosol, although *Arimoto et al.* [1996] proposed a few likely factors in controlling the ratio.

3.2. High Cl-Depletion of Marine Aerosols Over the SCS

[11] Relationships between sodium and chloride were examined for the dichotomous samples as shown in Figure 5a. Both sodium and chloride correlate well for coarse-mode aerosols with a mean Cl/Na mass ratio of 1.27, obviously lower than that (1.80) of bulk seawater, indicative of Cl-depletion. For fine-mode aerosols, however, no significant relationship can be found, and the Cl/Na mass ratios (average 0.22) are much lower than that of bulk seawater, revealing a more substantial Cl-depletion for fine-mode sea salt aerosols than for the coarse-mode fraction (Figure 5a). Here dust-derived sodium, that would theoretically release only an insignificant portion of water-soluble Na, is not taken into account since the concentrations of water-soluble Al (assuming that this element is a conclusive dust indicator that enables us to estimate the dust-derived soluble Na) are very low. To confirm that such low Cl/Na mass ratios are actually caused by Cl-depletion instead of Na enrichment, Mg/Na mass ratios were then examined. The resultant Mg/Na mass ratios for both coarse (0.11) and fine (0.11) mode samples are very close to the bulk seawater ratio (0.12, see Figure 5b), definitely suggestive of a sea spray origin. Furthermore, we tested whether it was the result of an artifact during sample collection [*Yao et al.*, 2003]. The first bin size (>18 μm) particles of two sets of size-resolved samples have Cl/Na concentration ratios near that of bulk seawater or somewhat higher, consistent with results of *Sellegri et al.* [2001]. This could provide evidence of no Cl-depletion for the first bin size (>18 μm) sea salt aerosols, and in turn suggested no artifact responsible for the observed chloride deficit. The explanation is that higher degrees of Cl-depletion would be expected to occur in the coarse-sized samples, as they were collected in the place next to the sampler's air stream inlet, if artificial biases did occur during sampling. It therefore can be concluded that high Cl-depletion did occur in marine aerosols of the SCS and that the Cl-depletion percentage ($\%Cl_{dep}$) can be calculated as follows [*Quinn et al.*, 2000]

$$\left([Cl^-_{ss}] - [Cl^-_{meas}]\right)/[Cl^-_{ss}] \times 100\% \tag{1}$$

where $[Cl^-_{ss}] = 1.80 \times [Na^+_{meas}]$ and $[Cl^-_{meas}]$ and $[Na^+_{meas}]$ are the measured Cl^- and Na^+ mass concentrations.

[12] The Cl-depletion obtained for dichotomous aerosol samples, as summarized in Table 2, reveals a size-dependent pattern with depletion levels much higher for fine-mode aerosols (~85%) than for coarse-mode aerosols (~30%). Notably, the Cl-depletion for the fine-mode aerosols reached a constantly high value of about 95% (i.e., nearly complete Cl-depletion) if the two samples collected on cloudy days were excluded from consideration. For the size-resolved samples the size-dependent pattern is much more obvious, as depicted in Figure 4c. Even though Cl^- concentrations for the last four (i.e., <0.56 μm for the November 2004 samples) or six stages (i.e., <1.8 μm for the January 2005 samples) of subsamples are below detection limits (~2 ng/m^3), their likely maximum concentrations of Cl^- are still much lower than the expected Cl^- concentrations corresponding to the measured Na concentrations, considering analytical uncertainties. Thus these fine subsamples could be treated as having nearly complete Cl-depletion (i.e., 100%), in agreement with the results of the fine-mode dichotomous samples (Figure 4c) and also with the results of *Kerminen et al.* [1998] from a contrasting environment, the Arctic Ocean. The size dependence of Cl-depletion in our study is rather consistent with results obtained from many coastal and remote ocean sites while the magnitude of Cl-depletion, especially for the fine-mode fraction, appears much higher [*Yao et al.*, 2003].

[13] Moreover, relationships of equivalent concentration ratios between $[Cl^- + NO_3^-]$ and Na^+ were also examined,

Table 2. Cl-Depletion Percentage for Dichotomous Samples Collected From the Northern South China Sea on Two Research Cruises Conducted in November 2004 and January 2005

	November 2004		January 2005	
Sample	$PM_{2.5-10}$	$PM_{2.5}$	$PM_{2.5-10}$	$PM_{2.5}$
1	37	96	25	99
2	25	99	25	55
3	29	94	32	100
4	30	98	25	100
5	26	46		
6	39	97		
Mean ± S.D.	30 ± 6	85 ± 21	27 ± 4	86 ± 23

Table 3. A Comparison of Cl-Depletion in Marine Aerosols

Region/Season	Sample Type	Cl-Depletion Percentage	Species Accounting for the Acid Displacement	Reference
South China Sea/winter monsoon	both coarse (>2.5 μm) and fine (<2.5 μm) aerosols	86% for fine-mode and 29% for coarse-mode aerosols; 98% for fine-mode and 30% for coarse-mode aerosols excluding two cloudy samples	nss sulfate for fine- and nitrate for coarse-mode aerosols	this work
Jeju Island off southern Korea/spring (East Asia)	both coarse (>2.49 μm) and fine (<2.49 μm) aerosols	during Asian dust period 40% for fine-mode and 13% for coarse-mode aerosols, while during the non-Asia dust period 55% for fine-mode and 16% for coarse-mode aerosols[a]	not clearly specified	*Park et al.* [2004]
NE Pacific Ocean/varying seasons	>1.6 μm size-segregated aerosols	~3%[b]	nitrate	*Newberg et al.* [2005]
East coast of United States (Bermuda)/spring	size-segregated aerosols	~14%	nitrate	*Keene and Savoie* [1998]
Tropical northern Atlantic Ocean/spring	both coarse (>3 μm) and fine (<3 μm) aerosols	29.7 ± 9.9% for fine mode and 11.9 ± 13.3% for coarse mode	Nss sulfate for fine-mode and nitrate for coarse-mode aerosols	*Johansen et al.* [2000]
Tropical Arabian Sea (northern Indian Ocean)/late spring and summer	(not specified)	3.5 ± 6.3% in the SW monsoon and 15 ± 9% in the intermonsoon	both nss sulfate and nitrate	*Johansen et al.* [1999]
Tropical Arabian Sea/spring	both coarse (>3 μm) and fine (<3 μm) aerosols	89 ± 9% for fine-mode and 25.6 ± 21.3% for coarse-mode aerosols	Nss sulfate for fine-mode and nitrate for coarse-mode aerosols	*Johansen and Hoffmann* [2004]
NW Mediterranean Sea	size-segregated aerosols	18.5 ± 14.5%	mostly nitrate and occasionally nss sulfate	*Sellegri et al.* [2001]
Artic/winter and spring	coarse (>2.3 μm) and fine (<2.3 μm) mode aerosols	no Cl-depletion for coarse-, but nearly completed depletion for fine-mode aerosols	mainly sulfate	*Hara et al.* [2002]
Antarctic coastal site/varying seasons	bulk aerosols	10% in summer and no depletion in winter	mainly nitrate	*Jourdain and Legrand* [2002]

[a] Calculated from the reported Cl/Na mass ratios.
[b] Calculated from the reported enrichment factor of chloride.

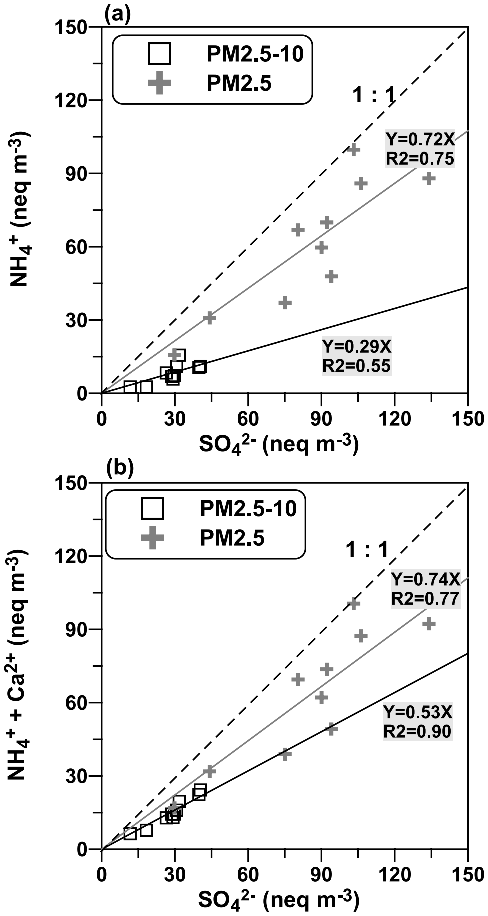

Figure 6. Relationships between NH_4^+ and SO_4^{2-} (a) and between [NH_4^+ + Ca^{2+}] and SO_4^{2-} (b) for two modes of aerosols.

as illustrated in Figure 5c. The mean ratio (0.94) for the two species is almost 1.0 for coarse-mode aerosols, revealing that coarse-mode nitrate may form onto the sea salt, essentially through acid displacement between nitric acid and deliquesced sea salt [*Eriksson*, 1959, 1960; *Quinn and Bates*, 2005], which can be represented by

$$HNO_{3(g)} + NaCl_{(aq)} \rightarrow NaNO_{3(aq)} + HCl_{(g)} \qquad (2)$$

[14] Such a reaction has been well demonstrated to be predominantly responsible for chloride losses in coarse sea salt aerosols in the marine boundary layer. Nevertheless, the [Cl^- + NO_3^-] to Na^+ mean ratio (0.17) in fine-mode aerosols is still lower than unity (inset of Figure 5c), indicating that additional ionic species other than nitrate is essentially responsible for Cl displacement of fine sea salt, but there are two exceptional data points that are closer to 1.0 (inset of Figure 5c). The two samples with lower Cl-depletion were collected on a cloudy/rainy day on each cruise. This indicates that Cl-depletion is more severe for fine-mode than for coarse-mode aerosols and is more active during a sunny day than during a rainy/cloudy day. This further suggests that Cl-depletion is, at least to some extent, related to photochemical reactions [*Pósfai et al.*, 1995; *Pszenny et al.*, 2004], which is discussed section 3.3.

[15] Calculating the charge balance of cations and anions can give clues regarding reactions between acidic gases and the primary natural particles, such as sea salt and mineral dust. Relationships of equivalent concentration ratios between total anions [Cl^- + NO_3^- +SO_4^{2-}] and total cations [Na^+ + Mg^{2+} + Ca^{2+} + K^+ + NH_4^+] were further examined, as depicted in Figure 5d. The ratios generally follow the 1:1 ratio, not only for the coarse mode (0.89) but also for the fine mode (0.85). This suggests that SO_4^{2-} substitution could account for Cl-depletion of the fine-mode sea salt aerosols through the following equation:

$$H_2SO_{4(g)} + 2NaCl_{(aq)} \rightarrow Na_2SO_{4(aq)} + 2HCl_{(g)} \qquad (3)$$

in which H_2SO_4 may form from oxidation of gaseous SO_2. The mean values of total anions to total cations equivalent ratios especially for fine-mode aerosols are somewhat lower than 1.0, which probably is a result of excluding the carbonate (and/or bicarbonate) and organic anions in the total anions [*Maxwell-Meier et al.*, 2004]. In addition to reactions between acidic gases and sea salt, some other processes such as cloud and aging processing have also been proposed to cause a Cl-deficit in marine aerosols [*Song and Carmichael*, 1999; *Yao et al.*, 2003].

3.3. Controlling Factors of Cl-Depletion: Air Pollution and Photochemistry

[16] Compared to many coastal and remote oceans, the Cl-depletion measured in marine aerosols of the tropical SCS is apparently more substantial (Table 3). Chloride depletion is size-dependent; fine particles show a higher Cl-depletion, and coarse particles show a lower Cl-depletion. The combined findings of high Cl-depletion and high sulfate concentrations associated with fine-mode aerosols over the SCS imply that the study region is substantially influenced by SO_2-rich air pollution from fossil fuel combustion (particularly coal combustion), mainly from the China continent [*Streets et al.*, 2000; *Carmichael et al.*, 2002] and biomass burning, mainly from Southeast Asia [*Arndt et al.*, 1997]. This inference is fully supported by chemical measurements [*Wang et al.*, 2005] and also by model simulations [*Liu et al.*, 2005], showing that the ocean studied is one of the worldwide hot spots of sulfuric species pollution. In the eastern Mediterranean, Cl-deficit was observed only in the polluted summer but not in the clean winter [*Bardouki et al.*, 2003], revealing that it is strongly related to air pollution [*Pósfai et al.*, 1995; *Niemi et al.*, 2005]. However, compared with the East Asia coastal regions like the ECS similarly under the influence of Asian outflow, the SCS has the higher magnitudes of Cl-deficit (Table 3). Contrarily, the ECS received much more Asian outflow of acidic gases (e.g., NO_x, HNO_3, and SO_2) than did the SCS. This may suggest that the strength of emissions of acid gases would not be the most (or only) critical controlling factor of Cl-deficit, which is consistent with the suggestion of *Johansen et al.* [1999].

[17] A marked feature is that acid displacement for the coarse-mode particles was caused almost solely by NO_3^- substitution, dissimilar to the common cases of coastal and remote oceans in which both NO_3^- and SO_4^{2-} are similarly responsible for Cl-depletion [*Sievering et al.*, 1992; *Carmichael et al.*, 1996; *Zhuang et al.*, 1999]. Also,

the results are different from the cases observed at coastal sites around East Asia [*Zhuang et al.*, 1999; *Zhang et al.*, 2003], where the uptake of acidic gases is dominated usually by dust particles but not sea salt. Interestingly, only nitrate rather than both nitrate and sulfate substitutions were also suggested to account for Cl-deficit of sea salt particles in the Arctic [*Hara et al.*, 1999], a contrasting environment to the study region, the tropical SCS. For the fine-mode aerosols, NO_3^- substitution cannot explain the anomalous Cl-depletion alone, and SO_4^{2-} substitution needs to be taken into account. This suggests a continental influence [*Niemi et al.*, 2005] and the aging process of aerosols [*Song and Carmichael*, 1999], which could be confirmed by the air mass backward trajectory analysis (Figure 3), illustrating that the continental air parcel from northern China has traveled great distances to the study area.

[18] Moreover, relationships between NH_4^+ and $_{nss}SO_4^{2-}$ with equivalent ratios of 0.72 for fine-mode aerosols (Figure 6a), even lower than that observed at an island site in the ECS [*Takami et al.*, 2005], suggest that the two ions may mainly be in the form of NH_4HSO_4, with an acidic nature, instead of $(NH_4)_2SO_4$. When additionally considering Ca, particularly for coarse particles (Figure 6b), the $[NH_4^+ + Ca^{2+}]/SO_4^{2-}$ ratio of 0.53 ($R^2 = 0.90$) is larger than the NH_4^+/SO_4^{2-} ratio of 0.29 ($R^2 = 0.55$) and, more importantly, their correlation becomes much better (Figure 6b). It reveals that most coarse sulfate aerosols may be present in the forms of NH_4HSO_4 and $CaSO_4$, accounting at least for over half of total SO_4^{2-}. In the case of fine-mode aerosols the $[NH_4^+ + Ca^{2+}]/SO_4^{2-}$ ratio is 0.74 (Figure 6b), somewhat larger than the NH_4^+/SO_4^{2-} ratio (0.72, Figure 6a) and still lower than 1. This indicates that sulfur-containing gases in the air of the SCS are likely sufficient to thoroughly react with NH_3 (ammonium sulfate then condensing onto preexisting fine particles), and fine-mode sea salt particles as well as a small amount of dust, which is in good agreement with the atmospheric measurements of trace gases [*Wang et al.*, 2005]. In the case of nitric acid it would fully react with coarse-mode sea salt particles.

[19] Additionally, Asian dust rich in Ca (or $CaCO_3$ mineral) uptakes sulfuric acid and internally mixes with sulfate when dispersed dust plumes meet SO_2-rich pollution, which is commonly observed in and around downstream regions [*Maxwell-Meier et al.*, 2004; *Matsumoto et al.*, 2006]. The presence of coarse-mode $CaSO_4$ (e.g., gypsum) observed may indicate again that the SCS air is aged, significantly containing acidic pollutants of terrestrial origins. *Quinn and Bates* [2005] found that the Cl to Na mass ratio was closer to that of bulk seawater in dusty periods than during polluted periods because of the buffering capability of dust particles. During the study period the levels of dust aerosols over the SCS are low, based on the results of low dust-derived Al measured (not shown), and this perhaps leads to a low Cl/Na ratio (i.e., high Cl-depletion) of marine aerosols in the absence of the buffering capability of dust particles.

[20] Another interesting feature is that fine-mode chloride almost disappears from sea salt, except for the two samples collected during rainy/cloudy days (Table 2) when these samples had the highest fine-mode NO_3^- and lowest $_{nss}SO_4^{2-}$ (also NH_4^+) (Figures 2b and 2d). Nevertheless, in contrast to the fine-mode samples collected on the same (rainy/cloudy) days, the two coarse-mode samples had relatively constant Cl depletion (∼25%), close to those observed on most (sunny) days (Table 2). However, lower Cl-depletion in the two fine-mode aerosols essentially did not result from the wet scavenging process, based on the observed increase in NO_3^- concentrations. This may be explained by two possible reasons: the combination of reduction in the sulfur-containing pollutants and changes in the relative contribution between aged and fresh marine aerosols [*Song and Carmichael*, 1999] and the photochemical process [*Pósfai et al.*, 1995; *Pszenny et al.*, 2004]. Showers would result in a wet scavenging effect, subsequently leading to the decline of anthropogenic contributions such as sulfate aerosols, SO_2 and NH_3 through long-range transport from the land, as illustrated by the temporal variability of the fine-mode NO_3^- and $_{nss}SO_4^{2-}$ (Figures 2b and 2d). Alternatively, the marine boundary layer could have become cleaner and the relative proportions of aged and fresh marine aerosols changed. Consequently, this could have affected the uptake and then partitioning of sulfuric and nitric acids on deliquesced sea salt, and then promoted the fine nitrate production. *Pósfai et al.* [1995] observed a complete displacement of Cl^- by NO_3^- in sea salt during the day and suggested that it is governed by a photochemical reaction. This reaction may be related to the daytime formation of HNO_3 from NO_2 and photochemically produced OH. *Mamane and Gottlieb* [1992] showed that sea salt reacts with HNO_3 and NO_2 much faster under UV irradiation than in the dark. Accordingly, the cloudy case is, to a certain extent, similar to the nighttime case. *Sellegri et al.* [2001] also found that Cl-depletion was limited under rainy conditions. These related processes are more significant for the fine-mode sea salt. Meanwhile, the change in relative humidity seems to be involved in acid displacement of sea salt [*Maxwell-Meier et al.*, 2004]. So far there are only small data sets regarding the role of cloud or sunlight, so we cannot deal with the observations in detail, which need sufficient data sets in the future to demonstrate these roles.

4. Concluding Remarks

[21] Marine aerosols from the tropical SCS are characterized by high levels of anthropogenic species such as $_{nss}SO_4^{2-}$ and NH_4^+ when compared to remote open oceans and by a high $_{nss}SO_4^{2-}/NO_3^-$ ratio when compared to those observed over the western Pacific Ocean. Also they show a high degree of Cl-depletion, which could result from acid displacement of sea salt with nitric and sulfuric acids. Nevertheless, coarse- and fine-mode sea salt aerosols behave in two different fashions, the former favoring a reaction with nitric acid and the latter favoring a reaction with sulfuric acid. The distinct partitioning between fine- and coarse-mode sea salt for NO_3^- and $_{nss}SO_4^{2-}$ may be responsible, at least in part, for the high $_{nss}SO_4^{2-}/NO_3^-$ ratios in the SCS marine aerosols because coarse nitrate is more preferentially removed through dry deposition than fine sulfate.

[22] The degree of Cl-deficit was size-dependent, increasing with decreasing particle sizes. Chlorine release is suggested to reflect the changes in the chemical compositions of sea salt particles when they encountered the advecting polluted continental air. Moreover, photochemical

reactions may play a role in triggering the liberation of chorine from sea salt. The marginal seas around the Asian continent, where there is rapid industrialization and urbanization, provide an ideal natural setting to examine the chemical reactions between natural particles (e.g., dust and sea salt) and gaseous pollutants (e.g., sulfuric and reactive oxidative nitrogen species). This is particularly the case for the East and South China Seas, which are exposed to air masses polluted by anthropogenic activities such as biomass burning and industrial emissions in southern China and South/Southeast Asia. Thus the subject merits additional investigation to characterize the physicochemical properties of marine aerosols in the tropical/subtropical South China Sea, which would facilitate the model simulations of atmospheric chemistry and climate forcing.

[23] **Acknowledgments.** We thank the anonymous reviewers for their constructive suggestions and comments. We also thank the technicians and crew of R/V *Ocean Researcher I* and National Center of Oceanographic Research of Taiwan for assistance with sampling. The authors gratefully acknowledge the NOAA Air Resources Laboratory (ARL) for the provision of the HYSPLIT transport and dispersion model and READY Web site (http://www.arl.noaa.gov/ready.html) used in this publication. We also would like to acknowledge the IGAC for their moral support. This work was supported by National Science Council (R.O.C.) grants NSC 94-2611-M001-002 and NSC 95-2611-M001-001 and partly by the Center for Marine Bioscience and Biotechnology, NTOU, to S.C.H.

References

Arimoto, R., R. A. Duce, D. L. Savoie, J. M. Prospero, R. Talbot, J. D. Cullen, U. Tomza, N. F. Lewis, and B. J. Jay (1996), Relationships among aerosol constituents from Asia and the North Pacific during PEM-West A, *J. Geophys. Res.*, *101*, 2011–2023.

Arndt, R. L., G. R. Carmichael, D. G. Streets, and N. Bhatti (1997), Sulfur dioxide emissions and sectorial contributions to sulfur deposition in Asia, *Atmos. Environ.*, *31*, 1553–1572.

Bardouki, H., H. Liakakou, C. Economou, J. Sciare, J. Smolik, V. Zdimal, K. Eleftheriadis, M. Lazaridis, C. Dye, and N. Mihalopoulos (2003), Chemical composition of size-resolved atmospheric aerosols in the eastern Mediterranean during summer and winter, *Atmos. Environ.*, *37*, 195–208.

Bates, T. S., et al. (2004), Marine boundary layer dust and pollutant transport associated with the passage of a frontal system over eastern Asia, *J. Geophys. Res.*, *109*, D19S19, doi:10.1029/2003JD004094.

Carmichael, G. R., Y. Zhang, L. L. Chen, M. S. Hong, and H. Ueda (1996), Seasonal variation of aerosol composition at Cheju Island, Korea, *Atmos. Environ.*, *30*, 2407–2416.

Carmichael, G. R., D. G. Streets, G. Calori, M. Amann, M. Z. Jacobson, J. Hansen, and H. Ueda (2002), Changing trends in sulfur emissions in Asia: Implications for acid deposition, air pollution, and climate, *Environ. Sci. Technol.*, *36*, 4707–4713.

Eriksson, E. (1959), The yearly circulation of chloride and sulfate in nature; meteorological, geochemical, and pedological implications: Part I, *Tellus*, *11*, 375–403.

Eriksson, E. (1960), The yearly circulation of chloride and sulfate in nature; meteorological, geochemical, and pedological implications: Part II, *Tellus*, *12*, 63–109.

Fan, S. M., and D. J. Jacob (1992), Surface ozone depletion in Arctic spring sustained by bromine reactions on aerosol, *Nature*, *359*, 522–524.

Hara, K., K. Osada, M. Hayashi, K. Matsunaga, T. Shibata, and Y. Iwasaka (1999), Fractionation of inorganic nitrates in winter Arctic troposphere: Coarse aerosol particles containing inorganic nitrates, *J. Geophys. Res.*, *104*, 23,671–23,679.

Hara, K., K. Osada, K. Matsunaga, Y. Iwasaka, T. Shibata, and K. Furuya (2002), Atmospheric inorganic chlorine and bromine species in Arctic boundary layer of the winter/spring, *J. Geophys. Res.*, *107*(D18), 4361, doi:10.1029/2001JD001008.

Hsu, S. C., S. C. Liu, C. Y. Lin, R. T. Hsu, Y. T. Huang, and Y. W. Chen (2004), Metal compositions and characterizations of PM10 and PM2.5 aerosols in Taipei during the springtime, 2002, *Terres. Atmos. Ocean. Sci.*, *15*, 925–948.

Hsu, S. C., S. C. Liu, W. L. Jeng, C. C. K. Chou, R. T. Hsu, Y. T. Hung, and Y. W. Chen (2006), Lead isotope ratios in ambient aerosols from Taipei, Taiwan: Identifying long-range transport of airborne Pb from the Yangtze Delta, *Atmos. Environ.*, *40*, 5393–5404.

Jobson, B. T., H. Niki, Y. Yokouchi, J. Bottenheim, F. Hopper, and R. Leaitch (1994), Measurements of C2–C6 hydrocarbons during the Polar Sunrise 1992 Experiment: Evidence for Cl atom and Br atom chemistry, *J. Geophys. Res.*, *99*, 25,355–25,368.

Johansen, A. M., and M. R. Hoffmann (2004), Chemical characterization of ambient aerosol collected during the northeast monsoon season over the Arabian Sea: Anions and cations, *J. Geophys. Res.*, *109*, D05305, doi:10.1029/2003JD004111.

Johansen, A. M., R. L. Siefert, and M. R. Hoffmann (1999), Chemical characterization of ambient aerosol collected during the southwest monsoon and intermonsoon seasons over the Arabian Sea: Anions and cations, *J. Geophys. Res.*, *104*, 26325–26347.

Johansen, A. M., R. L. Siefert, and M. R. Hoffmann (2000), Chemical composition of aerosols collected over the tropical North Atlantic Ocean, *J. Geophys. Res.*, *105*, 15277–15312.

Jourdain, B., and M. Legrand (2002), Year-round records of bulk and size-segregated aerosol composition and HCl and HNO_3 levels in the Dumont d'Urville (coastal Antarctica) atmosphere: Implications for sea-salt aerosol fractionation in the winter and summer, *J. Geophys. Res.*, *107*(D22), 4645, doi:10.1029/2002JD002471.

Keene, W. C., and D. L. Savoie (1998), The pH of deliquesced sea-salt aerosol in polluted marine air, *Geophys. Res. Lett.*, *25*, 2181–2184.

Kerminen, V. M., K. Teinila, R. Hillamo, and T. Pakkanen (1998), Substitution of chloride in sea-salt particles by inorganic and organic anions, *J. Aerosol Sci.*, *29*, 929–942.

Liu, X., J. E. Penner, and M. Herzog (2005), Global modeling of aerosol dynamics: Model description, evaluation, and interactions between sulfate and nonsulfate aerosols, *J. Geophys. Res.*, *110*, D18206, doi:10.1029/2004JD005674.

Ma, Q., M. Hu, T. Zhu, L. Liu, and M. Dai (2005), Seawater, atmospheric dimethylsulfide and aerosol ions in the Pearl River Estuary and the adjacent northern South China Sea, *J. Sea Res.*, *53*, 131–145.

Ma, Y., et al. (2003), Characteristics and influence of biosmoke on the fine-particle ionic composition measured in Asian outflow during the Transport and Chemical Evolution Over the Pacific (TRACE-P) experiment, *J. Geophys. Res.*, *108*(D21), 8816, doi:10.1029/2002JD003128.

Mamane, Y., and J. Gottlieb (1992), Nitrate formation on sea-salt and mineral particles: A single cell approach, *Atmos. Environ.*, *26*, 1763–1769.

Matsumoto, J., K. Takahashi, Y. Matsumi, A. Yabushita, A. Shimizu, I. Matsui, and N. Sugimoto (2006), Scavenging of pollutant acid substances by Asian mineral dust particles, *Geophys. Res. Lett.*, *33*, L07816, doi:10.1029/2006GL025782.

Matsumoto, K., I. Nagao, H. Tanaka, H. Miyaji, T. Iida, and Y. Ikebe (1998), Seasonal characteristics of organic and inorganic species and their size distributions in atmospheric aerosols over the northwest Pacific Ocean, *Atmos. Environ.*, *32*, 1931–1946.

Maxwell-Meier, K., R. Weber, C. Song, D. Orsini, Y. Ma, G. R. Carmichael, and D. G. Streets (2004), Inorganic composition of fine particles in mixed mineral dust-pollution plumes observed from airborne measurements during ACE-Asia, *J. Geophys. Res.*, *109*, D19S07, doi:10.1029/2003JD004464.

Nakamura, T., K. Matsumoto, and M. Uematsu (2005), Chemical characteristics of aerosols transported from Asia to the East China Sea: An evaluation of anthropogenic combined nitrogen deposition in autumn, *Atmos. Environ.*, *39*, 1749–1758.

Newberg, J. T., B. M. Matthew, and C. Anastasio (2005), Chloride and bromide depletions in sea-salt particles over the northeastern Pacific Ocean, *J. Geophys. Res.*, *110*, D06209, doi:10.1029/2004JD005446.

Niemi, J. V., H. Tervahattu, A. Virkkula, R. Hillamo, K. Teinilä, I. K. Koponen, and M. Kulmala (2005), Continental impact on marine boundary layer coarse particles over the Atlantic Ocean between Europe and Antarctica, *Atmos. Res.*, *75*, 301–321.

Park, S. H., C. B. Song, M. C. Kim, S. B. Kwon, and K. W. Lee (2004), Study on size distribution of total aerosol and water-soluble ions during an Asian dust storm event at Jeju Island, Korea, *Environ. Monit. Assess.*, *93*, 157–183.

Pósfai, M., J. R. Anderson, and P. R. Buseck (1995), Compositional variations of sea-salt-mode aerosol particles from the North Atlantic, *J. Geophys. Res.*, *100*, 23,063–23,074.

Prospero, J. M., and D. L. Savoie (2003), Long-term record of nss-sulfate and nitrate in aerosols on Midway Island, 1981–2000: Evidence of increased (now decreasing?) anthropogenic emissions from Asia, *J. Geophys. Res.*, *108*(D1), 4019, doi:10.1029/2001JD001524.

Pszenny, A. A. P., J. Moldanová, W. C. Keene, R. Sander, J. R. Maben, M. Martinez, P. J. Crutzen, D. Perner, and R. G. Prinn (2004), Halogen cycling and aerosol pH in the Hawaiian marine boundary layer, *Atmos. Chem. Phys.*, *4*, 147–168.

Quinn, P. K., and T. S. Bates (2005), Regional aerosol properties: Comparisons of boundary layer measurements from ACE 1, ACE 2, Aerosols99, INDOEX, ACE Asia, TARFOX, and NEAQS, *J. Geophys. Res.*, *110*, D14202, doi:10.1029/2004JD004755.

Quinn, P. K., T. S. Bates, D. J. Coffman, T. L. Miller, J. E. Johnson, D. S. Covert, J.-P. Putaud, C. Neusüß, and T. Novakov (2000), A comparison of aerosol chemical and optical properties from the 1st and 2nd Aerosol Characterization Experiments, *Tellus, Ser. B*, *52*, 239–257.

Sellegri, K., J. Gourdeau, J. P. Putaud, and S. Despiau (2001), Chemical composition of marine aerosol in a Mediterranean coastal zone during the FETCH experiment, *J. Geophys. Res.*, *106*, 12,023–12,037.

Sievering, H., J. Boatman, E. Gorman, Y. Kim, L. Anderson, G. Ennis, M. Luria, and S. Pandis (1992), Removal of sulphur from the marine boundary laver by ozone oxidation in sea-salt aerosols, *Nature*, *360*, 571–573.

Song, C. H., and G. R. Carmichael (1999), The aging process of naturally emitted aerosol (sea-salt and mineral aerosol) during long range transport, *Atmos. Environ.*, *33*, 2203–2218.

Streets, D. G., N. Y. Tsai, H. Akimoto, and K. Oka (2000), Sulfur dioxide emissions in Asia in the period 1985–1997, *Atmos. Environ.*, *34*, 4413–4424.

Sturges, W. T., and G. E. Shaw (1993), Halogens in aerosol in central Alaska, *Atmos. Environ.*, *27*, 2969–2977.

Takami, A., T. Miyoshi, A. Shimono, and S. Hatakeyama (2005), Chemical composition of fine aerosol measured by AMS at Fukue Island, Japan during APEX period, *Atmos. Environ.*, *39*, 4913–4924.

Vogt, R., P. J. Crutzen, and R. Sander (1996), A mechanism for halogen release from sea-salt aerosol in the remote marine boundary layer, *Nature*, *383*, 327–330.

Wang, T., H. Guo, D. R. Blake, Y. H. Kwok, I. J. Simpson, and Y. S. Li (2005), Measurements of trace gases in the inflow of South China Sea background air and outflow of regional pollution at Tai O, southern China, *J. Atmos. Chem.*, *52*, 295–317.

Yao, X., M. Fang, and C. K. Chan (2003), The size dependence of chloride depletion in fine and coarse sea-salt particles, *Atmos. Environ.*, *37*, 743–751.

Zhang, D., Y. Iwasaka, G. Shi, J. Zang, A. Matsuki, and D. Trochkine (2003), Mixture state and size of Asian dust particles collected at southwestern Japan in spring 2000, *J. Geophys. Res.*, *108*(D24), 4760, doi:10.1029/2003JD003869.

Zhuang, H., C. K. Chan, M. Fang, and A. S. Wexler (1999), Formation of nitrate and non-sea-salt sulfate on coarse particles, *Atmos. Environ.*, *33*, 4223–4233.

S.-C. Hsu, Y.-T. Huang, S.-J. Kao, S. C. Liu, F. Tsai, and J.-Y. Tu, Research Center for Environmental Changes, Academia Sinica, 128, Sec. 2, Academia Road, Nankang, Taipei 11529, Taiwan. (schsu815@rcec.sinica.edu.tw)

W.-L. Jeng and C.-M. Tseng, Institute of Oceanography, National Taiwan University, No. 1, Sec. 4, Roosevelt Road, Taipei 10617, Taiwan.

Y. Yang, National Center of Oceanographic Research, National Taiwan University, No. 1, Sec. 4, Roosevelt Road, Taipei 10617, Taiwan.